Surface structure and stress in Fe monolayers on W(110)

H. L. Meyerheim, D. Sander, R. Popescu, and J. Kirschner
Max-Planck-Institut für Mikrostrukturphysik, Weinberg 2, D-06120 Halle, Germany

P. Steadman and S. Ferrer
European Synchrotron Radiation Facility, Beamline ID-03, Boîte Postale 220, F-38043 Grenoble, France
(Received 10 January 2001; published 9 July 2001)

We present a surface x-ray structure analysis of Fe on W(110) deposited at room temperature in the coverage range up to 1.7 ML, in combination with *in situ* stress measurements. The maximum compressive stress is observed at about 0.7 ML, and coincides with the maximum first-layer Fe occupancy. Further island coalescence is inhibited. The onset of tensile stress at higher coverage is related with the growth of the second pseudomorphic Fe layer. At 1.2 ML only fractions of 0.70 ± 0.10 and 0.10 ± 0.10 ML of Fe, in the first and second layers, respectively, are located in pseudomorphic sites. At 1.7 ML three pseudomorphic Fe layers (with fractional ML occupancies of 0.80 ± 0.10, 0.60 ± 0.10, and 0.20 ± 0.10) have to be taken into account to fit the x-ray intensities indicating the growth of three-dimensional islands. The layer occupancies are consistent with scanning tunneling microscopy images. The Fe-W and Fe-Fe interlayer distances are compressed by up to 13% relative to the bulk distances, in good agreement with previous theoretical predictions and experiments.

DOI: 10.1103/PhysRevB.64.045414 PACS number(s): 68.35.Ct, 68.35.Gy, 68.55.Jk, 68.60.Bs

I. INTRODUCTION

For almost two decades the adsorption of Fe on W(110) has been one of the most intensely studied model systems in surface science.[1–21] On the one hand, this is due to its rich variety of reported peculiar magnetic properties, such as in- and out-of-plane anisotropy,[15] spin reorientation,[12,13] magnetic frustration,[8] and unusual domain wall pinning.[11] On the other hand, it is due to its outstanding mechanic and crystallographic properties.[16–18,20] The low-energy electron-diffraction (LEED) analysis of Gradmann and Waller[2] proposed that up to about a 2-ML coverage Fe grows pseudomorphically on W(110) (the coverage in ML is related to the W(110) surface atom density and is defined as 1.41×10^{15} Fe atoms per cm^2). At higher coverage, the formation of a regular array of misfit dislocations sets in as a result of the growing strain energy in the mismatched Fe layer. The misfit dislocations were also clearly identified by scanning tunneling microscopy (STM) investigations. However, pseudomorphic growth at low coverage cannot be directly identified by STM, because atomic resolution is lacking due to the low corrugation of the local density of states.[9,10] The surface mechanic properties were also investigated recently. The Fe/W(110) interface represents an adsorption system with a large lattice misfit of 9.4% ($a_W = 3.161$ Å, $a_{Fe} = 2.866$ Å), and does not show intermixing. Stress measurements during film growth have shown that up to about 0.6 ML there is compressive stress, which is in contrast to the expectation from strain considerations predicting tensile stress.[16,17,20] The stress measurements indicated that, already in the second layer, at a coverage of 1.2 ML a transition from pseudomorphic to nonpseudomorphic growth occurs.[20] Nevertheless, despite the intense efforts to determine the structure and properties of the Fe/W(110) interface in the low-coverage regime, quantitative structural data are very rare. Even for the pseudomorphic growth regime there have been only a few investigations concerned with a determination of the atomic arrangement at the interface and its correlation with magnetic and mechanical properties. Among the experimental investigations there is only the LEED analysis of Albrecht and co-workers[5,6] using a ''classical'' surface structure analysis technique, although the method to analyze the data originates from a kinematical approach to electron diffraction. A schematic view of the pseudomorphic Fe/W(110) structure is shown in Fig. 1. The authors of Refs. 5 and 6 six found, for the first Fe layer, a normal distance, d(Fe1-W1), of 1.94 Å, which corresponds to a contraction of 13% relative to the bulk W-layer spacing (2.23 Å). Furthermore, for the second-layer distance, d(Fe1-Fe2), a compression of 10% to 1.82 Å relative to the bulk Fe interlayer distance (2.03 Å) is found. Apart from this work, there is only the x-ray photoelectron diffraction (XPD) investigation of Tober *et al.*[14] which found a contraction of 7.2% for d(Fe1-W1). More recent theoretical work in Refs. 19 and 21 also reported large contractions. For d(Fe1-W1) these authors found values of 13% and 17%, respectively. Adding a second Fe layer (Fe2) partially relaxes this contraction to 10.6% and 13%, respectively. For d(Fe1-Fe2) the calculations predict contractions of 11.9% and 4.7%. Table I summarizes these results in comparison to our own findings, discussed below.

The discrepancies of the structural data that have been

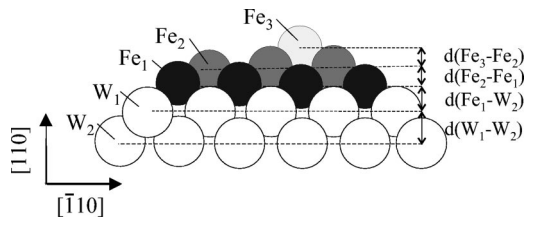

FIG. 1. Schematic picture of the Fe/W(110) interface assuming pseudomorphic growth. The interlayer spacings are labeled according to Table I.

TABLE I. Parameters for the pseudomorphic structure of Fe/W(110) as derived from experimental and theoretical investigations. The relative changes of the interlayer distances are given with respect to the bulk *W* distance of 2.23 Å for *d*(Fe1-W1) and *d*(W1-W2), and relative to the bulk Fe distance of 2.03 Å for *d*(Fe3-Fe2) and *d*(Fe2-Fe1).

	d(Fe3-Fe2)	*d*(Fe2-Fe1)	*d*(Fe1-W1)	*d*(W1-W2)	method	Ref.
experiment						
1.4 ML, 0.45 ML		−10%	−13%		LEED	5, 6
1.2 ML			−7.2%	+2.2%	XPD	14
1.2 ML		−13±2%	−8±2%	−1±1%	SXRD	this work
layer filling		$\theta=0.1\pm0.1$	$\theta=0.7\pm0.1$			
1.7 ML	−5±2%	−11±3%	−8±3%	−1±1%	SXRD	this work
layer filling	$\theta=0.1\pm0.1$	$\theta=0.6\pm0.1$	$\theta=0.8\pm0.1$			
theory						
1 ML			−12.9%	−0.1%	FP-LAPW[a]	19
2 ML		−11.9%	−10.6%	+0.03%	FP-LAPW	19
1 ML			−17%	−0.1%	FP-LMTO[b]	21
2 ML		−5%	−13%	+0.03%	FP-LMTO	21

[a]Full-potential-augmented plane wave.
[b]Full-potential linear muffin-tin orbital.

reported so far make an accurate analysis of the geometric interface structure as a function of Fe coverage highly desirable. To this end we performed surface x-ray diffraction (SXRD) experiments. SXRD has become a routinely applied technique for the structure determination of clean and adsorbate-covered surfaces, since the data analysis is based on the kinematic scattering theory which allows an easier interpretation of the measured intensities as compared to LEED.[22–24] In the present investigation we analyze the geometric structure of the Fe/W(110) interface in the pseudomorphic growth regime. SXRD has been carried out for two coverages of the Fe film (1.2 and 1.7 ML). In addition, during Fe deposition we have combined *in situ* monitoring of a surface x-ray reflection and the measurement of the surface stress. The surface stress was measured with an optical deflection technique to determine changes of the crystal curvature. This combination directly correlates surface structural properties with the corresponding stress in the surface layer. Since this study is limited to coverages below 2 ML no regular misfit dislocations have been formed yet. The structure analysis is based on the interpretation of the intensity distribution along the integer order crystal truncation rods (CTR's).[22–25]

The CTR's arise due to the truncation of the crystal, and can easily be treated theoretically by calculating the semi-infinite sum of the scattering contribution of the crystal lattice planes along the [110] direction. Neglecting absorption, this leads to the expression for the structure factor intensity $|F|^2=f_W^2/[4\sin^2(\pi/2(h+k+l)|2)]$ for the bulk truncated W(110) crystal in the primitive setting of the surface unit cell.[26] The detailed calculation shows that l is a continuous parameter, whereas h and k are integers. The atomic scattering factor for W is given by f_W, which is tabulated in Ref. 27. The CTR intensities are strongly peaked at the bulk Bragg condition $h+k+l=2n$, with n an integer, but are orders of magnitude smaller in between. For example, at the ''antiphase'' condition $h+k+l=2n+1$, one calculates $|F|^2=f_W^2/4$ and the scattered intensity equals 1/4 of a W monolayer. Surface layer relaxation and adsorbate coverages influence the scattered intensity in between the Bragg peaks. In the course of the structural analysis, these intensity changes are exploited to model the atomic structure of the surface region.

II. RESULTS AND DISCUSSION

The experiments were carried out at the beamline ID3 of the European Synchrotron Radiation Facility in Grenoble using a six-circle ultrahigh-vacuum diffractometer (base pressure 7×10^{-11} mbar) running in the *z*-axis mode.[28,29] The W(110) crystal with dimensions $12\times2\times0.1\,\mathrm{mm}^3$ was fixed at one end only, with clamps to allow free bending. The sample was cleaned by heating several times in 10^{-6}-mbar oxygen for 30 sec at 1500 °C. After a final 10-sec flash at 2000 °C, only minor traces (less than 1% of a ML) of carbon contamination could be detected by Auger-electron spectroscopy. Fe was deposited by electron-beam evaporation from a high purity Fe rod. Figure 2(a) shows the specular x-ray reflection intensity at the antiphase (001) scattering condition along the 00l CTR versus the Fe coverage. Simultaneously, the crystal curvature was measured. Surface stress changes induce a corresponding crystal bending which is detected by reflecting a laser beam onto a position sensitive detector as described in Ref. 17. The curvature of the crystal, from which the change of surface stress upon film growth can be deduced, is shown in Fig. 2(b). Initially, a compressive stress is found which is ascribed to the change of surface stress of W due to the adsorption of Fe.[20] At a coverage above 0.5 ML tensile stress due to the positive lattice mismatch between Fe and W is measured. The horizontal section of the stress curve in Fig. 2(b) indicates a slightly different curvature versus thickness behavior as compared to our previous studies,[16–18] where a reduced but not negligible slope was measured. We ascribe this to the lower growth rate (1 ML in 250 s) as

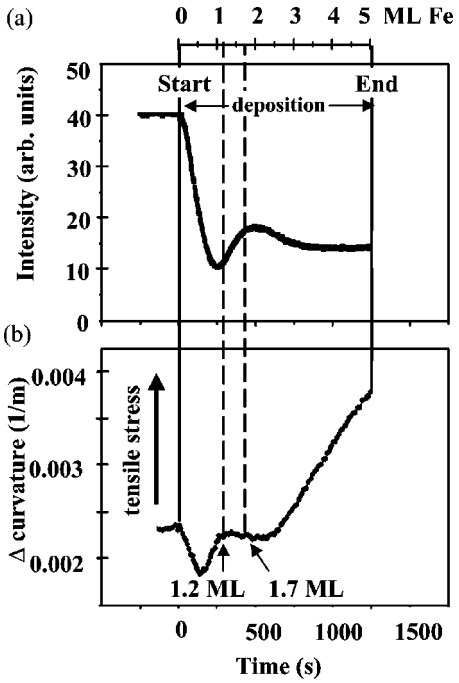

FIG. 2. (a) Specular SXRD reflection intensity at the (001) antiphase condition as a function of Fe coverage during deposition at 300 K. (b) Curvature measurement during Fe growth on W(110). The minimum of the curve indicates maximum compressive stress. CTR data were collected at 1.2 and 1.7 ML, as indicated by the dashed lines.

compared to our previous studies, which results in a more equilibrium like growth with lower stress.[18]

The nominal Fe coverage was calibrated independently by using a quartz oscillator. The x-ray reflection intensity exhibits a damped oscillating amplitude, characteristic for island growth. X-ray data sets were collected after termination of growth when the specular intensity was near the first minimum and maximum, as indicated by the dashed lines in Fig. 2. According to the simultaneous stress measurements (and the previous calibration) the amount of deposited Fe equals about 1.2 and 1.7 ML in these cases, respectively. The clear correlation between the calibration based on the interpretation of the SXRD intensity and the stress measurements is evident by a detailed inspection of Fig. 2. The kink of the stress curve (onset of misfit dislocations) at 1.2-ML coverage[20] occurs shortly after the first intensity minimum.

The latter is often qualitatively correlated with the completion of the first ML, because at this coverage there is the maximum antiphase scattering contribution by the pseudomorphic Fe adatoms. However, a short estimation shows that the minimum of the (001) intensity cannot be simply correlated with a complete first Fe layer. As outlined in Sec. I above, the total scattering intensity of the bulk W(110) crystal at the antiphase condition equals $f_W^2/4$. Adding a fraction of θ monolayers Fe in pseudomorphic sites on the W(110) surface yields, for the scattering amplitude, $|F_{001}|^2=|f_W/2-\theta f_{Fe}|^2$. Using $f_W=69$ and $f_{Fe}=23$ from Ref. 27, and assuming $\theta=1$, one obtains $|F_{001}|^2\approx 144$, which has to be compared to $|F_{001}|^2\approx 1225$ for clean W(110). This corresponds to about 11% of its initial value. In contrast, the observed intensity drop amounts to only 25%; see Fig. 2(a). This reduced drop in diffracted intensity can be ascribed to the growth of a second pseudomorphic layer before the first layer has been completed. The second layer contributes with an in-phase condition to the intensity, resulting in a smaller drop of intensity as compared to the oversimplified picture of a completed first layer. The detailed structure analysis discussed below supports this model conclusively.

Integrated x-ray reflection intensities were collected at a wavelength of 0.73 Å by transverse scans, i.e., by rotating the crystal about its surface normal while the x-ray incidence angle was kept fixed at 1.0° with respect to the sample surface. The large incidence angle (about six times the critical angle of total reflection) was chosen in order to avoid possible complications in the data analysis due to crystal bending. In the transverse direction the resolution is limited by the sample mosaic spread which was 0.1°. For each sample, several symmetrically independent CTR's were measured: $(01l)$ and $(20l)$ for 1.2-ML coverage and $(00l)$ and $(01l)$ for 1.7-ML coverage up to a maximum momentum transfer of $q_z=l\times c^*=4$ reciprocal lattice units.[26] The reciprocal-lattice parameter c^* is equal to 1.41 $(\text{Å})^{-1}$. In addition to these data sets, the corresponding CTR's of the uncovered sample were also measured. Thus the structure of the clean surface could be determined,[30] and they were used to normalize the integrated intensities (I) of the Fe-covered sample by evaluating the ratio (R) according to $R(q_z)=I_{cov}(q_z)/I_{cln}(q_z)$, where the subscripts (cov) and (cln) refer to covered and clean samples, respectively. The analysis of $R(q_z)$ avoids the consideration of correction factors in order to retrieve the structure factor intensities $|F(q_z)|^2$ from the integrated intensities.[31–33] In the present analysis the $|F(q_z)|^2$ data were derived from the integrated intensities by applying the Lorentz factor and the polarization factor. Furthermore, the intensity data were corrected for the effective sample area, which is the area illuminated by the x-ray beam and simultaneously intercepted by the detector. Especially in the present case, where a sample with a pronounced anisotropic shape with surface dimensions of 12×2 mm^2 is used, the analysis of $R(q_z)$ is a valuable test of the results obtained by fitting the $|F(q_z)|^2$ data. This is because the active sample area illuminated by the x-ray beam and intercepted by the detector rapidly varies with the different orientations of the sample and detector. Therefore the x-ray intensities are likely to be subject to large systematic errors. The ''ratio method'' was used successfully in some cases in the past,[34,35] and is well applicable where no substantial modification of the substrate surface is induced by adsorption. From previous STM and LEED investigations, it is known that this condition is fulfilled for Fe/W(110). The standard deviations σ of the intensities (and the ratios) were derived from the reproducibility of symmetry equivalent reflections and from the counting statistics.[22–24] In general, σ is in the 5–15 % range.

The solid symbols in Figs. 3 and 4 are the structure factor intensities $|F(q_z)|^2$ (upper panels) and the ratios $R(q_z)$ (lower panels). In the $|F(q_z)|^2$ data sets, solid squares represent the structure factor intensities for the uncovered samples, whereas the solid circles correspond to the Fe-

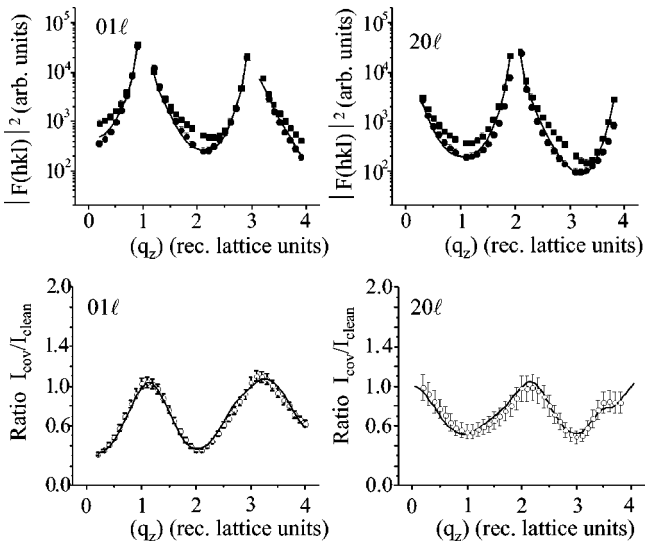

FIG. 3. Structure factor intensities $|F|^2$ (upper panels) measured along the $(01l)$ (left) and along the $(20l)$ CTR for the uncovered (solid squares) and 1.2-ML Fe-covered (solid circles) W(110) surfaces. The corresponding ratios between the Fe-covered W(110) and the clean W(110) are shown in the lower panels. Fits to the data are represented by solid lines.

covered ones. The lines are fits to the data (not shown for the rods of the uncovered sample). The derived structure parameters are compared in Table I with previous experimental and theoretical results. The error bars of the structure parameters are estimated from their variation depending on whether the parameters were derived from fits to the $|(F(q_z)|^2$ data or to the ratios. Already from qualitative inspection of $R(q_z)$, it is evident that, for the 1.2-ML Fe film, there is a major contribution only from one Fe layer. This leads to a simple sinusoidal shape of $R(q_z)$. In contrast, for the 1.7-ML sample, the more complicated behavior of $R(q_z)$ indicates the presence of several layers, i.e., island growth. Furthermore, all $R(q_z)$ data pass through values $R=1$ at the bulk Bragg reflections. This is because at the in-phase condition the intensity is dominated by the substrate scattering, making the adlayer contribution to the total scattering intensity negligible. A ratio $R=1$ at the in-phase condition is always indicative for the absence of systematic errors. In general, high-quality fits could be achieved as measured by the unweighted residuum, R_u.[36] For the $|(F(q_z)|^2$ data, R_u is in the 10–20 % range. For the $R(q_z)$ data it is between 3% and 10%.

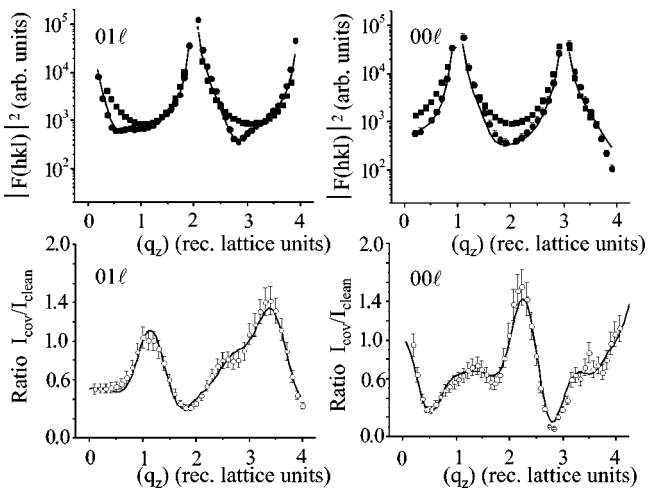

FIG. 4. Structure factor intensities $|F|^2$ and ratios for 1.7-ML Fe on W(110), as described in Fig. 3.

Our results are summarized as follows: In general, the contraction of the normal layer distances (Table I) is in fair agreement with previous experimental and theoretical work. In the pseudomorphic growth regime, large normal contractions are the consequence of the -9.4% misfit between Fe and W. Only a slight discrepancy exists between our results with previous work for d(Fe1-W1). The LEED analysis of Albrecht and co-workers,[5,6] and theoretical investigations, derived values in the range 10.6–17 %, respectively (the value 17% appears to be a bit outstanding as compared to the others, maybe due to the details of the theoretical approach). For both coverages we derive 8%, with a maximum error of 3%. On the other hand, a very good agreement—again with exception of Ref. 21—is obtained for the second (Fe2-Fe1) interlayer distance. Our analysis gives $13\pm2\%$ and $11\pm3\%$, in comparison with 10% determined by Albrecht *et al.*[5] and 11.9% by Qian and Hübner.[19] Pseudomorphic Fe/W(110) structures, including a third Fe layer, were not considered so far, either theoretically or experimentally. This can be attributed to the large computational difficulties associated with LEED or theoretical methods to deal with large systems. In contrast, our SXRD data of the 1.7-ML Fe film directly indicate the onset of third-layer growth in the pseudomorphic regime. Here the interlayer distance between the third and second Fe layers (Fe3-Fe2) is much less contracted (5%) than observed for the deeper layers (Table I). This rapid ''contraction damping'' can be attributed to the formation of small Fe clusters that become more bulklike with increasing thickness.

Although the error bar for the determination of the first substrate layer spacing $[d(\mathrm{W1\text{-}W2})]$ is large, there is some evidence for a residual contraction of $1\pm1\%$ after Fe deposition. In comparison with the uncovered sample for which we found a contraction of $2.7\pm0.5\%$,[30] this indicates that the substrate structure relaxes back upon Fe adsorption—though not completely, as predicted by theory (see Table I).

Even for 1.7-ML Fe there is no indication for the presence of a long-range ordered misfit dislocation network. The corresponding satellite reflections were observed only at higher coverage, and will be reported elsewhere.[37] This result might be surprising at first sight, as other techniques and the simultaneously taken curvature data indicate the end of pseudomorphic growth in the second layer, at a nominal coverage of 1.2 ML. Obviously, the initial stage of the structural change does not result in an ordered arrangement of Fe atoms in nonpseudomorphic sites.

There is some difference between the nominal coverage as calibrated by a quartz oscillator, and the total coverage as derived from the SXRD data. The latter is the sum of the fractional layer occupancies. In all cases the SXRD analysis yields less than the nominal coverage (0.8 ML versus 1.2 ML, and 1.6 ML versus 1.7 ML). Whereas for the latter the

discrepancy is within an error bar, for the lower coverage the difference might be explained by some fraction of disordered Fe. In addition, some macroscopic inhomogeneous Fe coverage on the sample surface cannot be excluded. For both samples a maximum first-layer Fe coverage of only 0.7–0.8 ML with an error bar of ± 0.10 ML is observed, indicating that the first pseudomorphic Fe layer is not completely filled. This supports previous STM analyses, also reporting an inhibited coalescence of the Fe islands at about 0.6 ML.[9] The hindered coalescence of the Fe islands might be caused by a relaxation of island edge atoms, which leads to lower strain energy for separated islands as compared to the closed film. Our finding of an incompletely filled first layer is also well in agreement with STM studies,[8,9] where even at coverages higher than 1.3 ML still some fraction of approximately 10% of the uncovered substrate is observed.

Island growth in the second and third layers can be qualitatively inferred from the rapid damping of the (001) intensity oscillations with increasing Fe coverage, as shown in Fig. 2(a). This is confirmed in more detail by the SXRD analysis of the 1.7-ML sample. A good fit to the data requires the assumption of a third layer occupied by a fractional coverage of 0.20 ± 0.10. This result is supported by the interpretation of STM images, such as the one shown in Fig. 5 for a 1.9-ML sample.[38] Black, gray, and bright areas correspond to the first, second, and third Fe layers. From a qualitative inspection of the image, Fe occupies fractions of about 70% and 20% of the surface area in the second and third layers, respectively.

Apart from these parameters, in addition surface roughness was taken into account. For the description of the roughness. Robinson[25] has developed an atomistic model assuming a geometric distribution of layer occupancies within the coherence length ($\approx$500 Å in the present case), where the layer occupancy is 1.0 for layer 0, β for layer 1, β^2 for layer 2, and so on. Increasing roughness leads to a steeper decrease of the CTR but not to an asymmetry of the intensity distribution as relaxation does. In general, values for β are in the range between 0.0 and 0.5, depending on the material and preparation. In general, semiconductor surfaces exhibit flatter surfaces than metals. For the clean W(110) surface we derived $\beta = 0.05(5)$, corresponding to a root mean square elevation of the surface of $\sigma = 0.5$ Å, which is a quite small value for a metal surface.[30] This was attributed to the high-temperature surface preparation. The roughness is only slightly enhanced upon Fe adsorption. We find values in the range between $\beta = 0.05$ and 0.15. In this context it should be noted that the surface roughness due to the Fe adsorbate atoms is inherently taken into account by the calculation of the CTR intensity by using fractional adlayer occupancies. Therefore, the only slight increase of β reflects that the W(110) surface does not become significantly rougher (e.g., due to an increased step density) upon Fe adsorption.

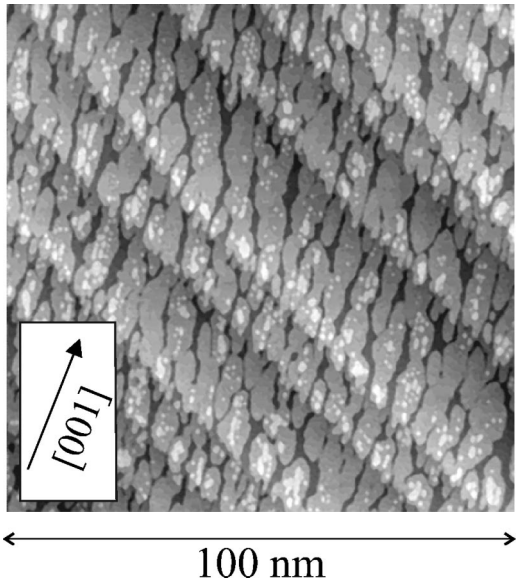

FIG. 5. STM image of 1.9-ML Fe deposited on W(110) at 300 K (Ref. 38). Monoatomic steps of the W substrate run from the upper left to the lower right side. Dark areas represent open patches in the second Fe layer, revealing Fe in the first layer. White areas correspond to Fe islands of the third layer.

In conclusion, we have presented a surface x-ray-diffraction analysis of the Fe/W(110) interface in the pseudomorphic growth regime. The interlayer contractions of 8%, 11%, and 5% for the first, second, and third layers, respectively, are in good agreement with theoretical predictions and previous work. We have no evidence of long-range ordered misfit dislocations at the maximum coverage of 1.7 ML that we investigated. The combination of the SXRD measurements with surface stress analysis has enabled us to correlate the onset of tensile stress in the Fe film with the beginning of second-layer growth. Further experiments are underway to investigate the correlation between film structure and film stress in more detail.

[1] G. Waller and U. Gradmann, Phys. Rev. B **26**, 6330 (1982).
[2] U. Gradmann and G. Waller, Surf. Sci. **116**, 539 (1982).
[3] S. Hong, A. Freeman, and C. Fu, Phys. Rev. B **38**, 12 156 (1988).
[4] M. Przybylski, I. Kaufmann, and U. Gradmann, Phys. Rev. B **40**, 8631 (1989).
[5] M. Albrecht, U. Gradmann, T. Reinert, and L. Fritsche, Solid State Commun. **78**, 671 (1991).
[6] M. Albrecht, Ph.D. thesis, Mathematisch-Naturwissenschaftliche Fakultät der Technischen Universität Clausthal, 1992.
[7] H. Elmers, J. Hauschild, H. Höche, U. Gradmann, H. Bethge, D. Heuer, and U. Köhler, Phys. Rev. Lett. **73**, 898 (1994).
[8] H. Elmers, J. Hauschild, H. Fritzsche, G. Liu, U. Gradmann, and U. Köhler, Phys. Rev. Lett. **75**, 2031 (1995).
[9] H. Bethge, D. Heuer, C. Jensen, K. Reshöft, and U. Köhler, Surf. Sci. **331–333**, 878 (1995).
[10] C. Jensen, K. Reshöft, and U. Köhler, Appl. Phys. A: Mater. Sci. Process. **62**, 217 (1996).
[11] D. Sander, R. Skomski, C. Schmidthals, A. Enders, and J. Kirschner, Phys. Rev. Lett. **77**, 2566 (1996).
[12] N. Weber, K. Wagner, H. Elmers, J. Hauschild, and U. Grad-

mann, Phys. Rev. B **55**, 14 121 (1997).
[13] T. Dürkop, H. Elmers, and U. Gradmann, J. Magn. Magn. Mater. **172**, L1 (1997).
[14] E. Tober, R. Ynzunza, F. Palomares, Z. Wang, Z. Hussain, M. van Hove, and C. Fadley, Phys. Rev. Lett. **79**, 2085 (1997).
[15] J. Hauschild, U. Gradmann, and H. Elmers, Appl. Phys. Lett. **72**, 3211 (1998).
[16] D. Sander, A. Enders, C. Schmidthals, D. Reuter, and J. Kirschner, Surf. Sci. **402–404**, 351 (1998).
[17] D. Sander, R. Skomski, A. Enders, C. Schmidthals, R. D., and J. Kirschner, J. Phys. D **31**, 663 (1998).
[18] D. Sander, Rep. Prog. Phys. **62**, 809 (1999).
[19] X. Qian and W. Hübner, Phys. Rev. B **60**, 16 192 (1999).
[20] D. Sander, A. Enders, and J. Kirschner, Europhys. Lett. **45**, 208 (1999).
[21] I. Galanakis, M. Alouani, and H. Dreyssé, Phys. Rev. B **62**, 3923 (2000).
[22] R. Feidenhans'l, Surf. Sci. Rep. **10**, 105 (1989).
[23] I. K. Robinson and D. J. Tweet, Rep. Prog. Phys. **55**, 599 (1992).
[24] H. Meyerheim and W. Moritz, Appl. Phys. A: Mater. Sci. Process. **67**, 645 (1998).
[25] I. K. Robinson, Phys. Rev. B **33**, 3830 (1986).
[26] We use a sample setting corresponding to a primitive $(p)1\times1$ surface unit cell, which is related to the bcc bulk setting by the relations: $[100]_p=1/2[\bar{1}11]_{\mathrm{bcc}}$, $[010]_p=1/2[\bar{1}\bar{1}1]_{\mathrm{bcc}}$, and $[001]_p=[110]_{\mathrm{bcc}}$.
[27] *International Tables for Crystallography*, edited by A. Wilson (Kluwer, Dordrecht, 1995), Vol. C.
[28] S. Brennan and P. Eisenberger, Nucl. Instrum. Methods Phys. Res. A **222**, 164 (1984).
[29] S. Ferrer and F. Comin, Rev. Sci. Instrum. **66**, 1674 (1994).
[30] H. Meyerheim, D. Sander, R. Popescu, P. Steadman, S. Ferrer, and J. Kirschner, Surf. Sci. **475**, 103 (2001).
[31] C. Schamper, H. Meyerheim, and W. Moritz, J. Appl. Crystallogr. **26**, 687 (1993).
[32] E. Vlieg, J. Appl. Crystallogr. **30**, 532 (1997).
[33] O. Robach, Y. Garreau, K. Aid, and M. Veron-Jolliot, J. Appl. Crystallogr. **33**, 1006 (2000).
[34] M. F. Toney, J. G. Gordon, M. G. Samant, G. L. Borges, O. R. Melroy, L. S. Kau, D. Wiesler, D. Yee, and L. B. Sorensen, Phys. Rev. B **42**, 5594 (1990).
[35] H. Meyerheim, J. Wever, V. Jahns, W. Moritz, P. J. Eng, and I. K. Robinson, Surf. Sci. **304**, 267 (1994).
[36] The unweighted residuum R_u is defined as $R_u=\Sigma\|F_{\mathrm{calc}}|-|F_{\mathrm{obs}}\|/\Sigma|F_{\mathrm{obs}}|$, where F_{obs} and F_{calc} are the observed and calculated structure factors, and the summation runs over all reflections.
[37] R. Popescu, H. Meyerheim, D. Sander, P. Steadman, S. Ferrer, and J. Kirschner (unpublished).
[38] C. Schmidthals, Ph.D. thesis, Martin-Luther Universität Halle-Wittenberg, Mathematisch-Naturwissenschaftlich-Technische Fakultät, 1997.